nature chemistry

ARTICLES

https://doi.org/10.1038/s41557-021-00665-7

Free-triplet generation with improved efficiency in tetracene oligomers through spatially separated triplet pair states

Zhiwei Wang[1,7], Heyuan Liu[2,7], Xiaoyu Xie[3,7], Chunfeng Zhang[1]✉, Rui Wang[1], Lan Chen[1], Yihe Xu[3], Haibo Ma[3]✉, Weihai Fang[3,4], Yao Yao[5], Hai Sang[1], Xiaoyong Wang[1], Xiyou Li[2]✉ and Min Xiao[1,6]✉

Singlet fission (SF) can potentially boost the efficiency of solar energy conversion by converting a singlet exciton (S_1) into two free triplets (T_1+T_1) through an intermediate state of a correlated triplet pair (TT). Although efficient TT generation has been recently realized in many intramolecular SF materials, their potential applications have been hindered by the poor efficiency of TT dissociation. Here we demonstrate that this can be overcome by employing a spatially separated ^{1}(T…T) state with weak intertriplet coupling in tetracene oligomers with three or more chromophores. By using transient magneto-optical spectroscopic methods, we show that free-triplet generation can be markedly enhanced through the SF pathway that involves the spatially separated ^{1}(T…T) state rather than the pathway mediated by the spatially adjacent TT state, leading to a marked improvement in free-triplet generation with an efficiency increase from 21% for the dimer to 85% (124%) for the trimer (tetramer).

Singlet fission (SF) can double the quantum efficiency of photocurrent generation by converting one photoexcited singlet exciton (S_1) into two triplet excitons (T_1+T_1)[1–6]. The theoretical limit of the power conversion efficiency in an ideal SF-based solar cell increases to ~45% from the ~33% found in a conventional single-junction device[7,8]. In terms of practical applications, intramolecular SF (iSF) materials, which can be naturally incorporated into the widely used device structure of the bulk heterojunction, have recently attracted rapidly growing interest[9–20]. SF has been widely described as a two-step process[1–3,21,22] with a key intermediate state of a spin-coherent correlated triplet pair (TT), that is, $S_1 \rightleftarrows TT \rightleftarrows T_1+T_1$. Nonetheless, the two steps exhibit different and sometimes conflicting dependences on the coupling between the two chromophores in iSF materials. In the widely studied dimer systems, the first step of triplet pair generation can be promoted by the interchromophore electronic interaction with optimal molecular orientations in covalently coupled chromophores[17,18,23–25]. However, such spatially proximate correlated triplet pairs may reduce the efficiency for the second process, that is, triplet pair dissociation into free triplets, for two reasons: (1) the strong spin–exchange interaction may slow down the spin dephasing of the TT state;[15,26] (2) the strong electronic coupling induces the processes of efficient triplet–triplet annihilation (TTA, including fusion of correlated triplet pair and annihilation of free triplets) that compete against the triplet separation process[11,19,27].

To circumvent the above dilemma, we propose to promote free-triplet generation amid iSF processes by making use of a spatially separated TT state (denoted as ^{1}(T…T)) in long oligomers with three or more chromophore units (Fig. 1). The concept of the spin-coherent ^{1}(T…T) state was originally proposed for intermolecular singlet fission (xSF) materials[5,21,28,29] to connect the proximately coupled adjacent TT state (^{1}(TT)) and free triplet states (T_1). Compared with the ^{1}(TT) state, the intertriplet coupling at the ^{1}(T…T) state with two spin-correlated triplets residing at a larger distance is much weaker. The role of this ^{1}(T…T) state during iSF processes remains rarely explored because such a ^{1}(T…T) state does not normally exist in the widely studied dilute solution of dimer systems with only two adjacent molecules (Fig. 1a)[9–19,30]. However, in a covalently linked trimer or a larger array (Fig. 1b) ^{1}(T…T) states may be formed with two triplets on non-adjacent units. In this case, the fusion processes (TTA of correlated triplet pair) will be markedly reduced and the spin dephasing will be promoted because of the reduced intertriplet coupling for the ^{1}(T…T) state, which will substantially improve the efficiency of free-triplet generation.

To experimentally verify the above hypothesis, we systematically study the different dynamics of the ^{1}(TT) and ^{1}(T…T) states during the iSF processes in a series of covalently linked tetracene oligomers (that is, tetracene dimer, trimer and tetramer; Fig. 1c) by employing transient magneto-optical spectroscopic methods. Normally, it is difficult to distinguish the ^{1}(TT) and ^{1}(T…T) states in SF materials by optical spectroscopy because of their heavily overlapped spectral features. We circumvent this issue by considering the different magnetic field effects (MFEs) for these two intermediate states. Because the intertriplet spin–exchange interaction is weaker at the ^{1}(T…T) state, the MFE for the ^{1}(T…T) state is markedly stronger than that for the ^{1}(TT) state in the low-field regime[26,31,32]. Therefore, the

[1]National Laboratory of Solid State Microstructures, School of Physics and Collaborative Innovation Center of Advanced Microstructures, Nanjing University, Nanjing, China. [2]School of Materials Science and Engineering, Institute of New Energy, China University of Petroleum (East China), Qingdao, China. [3]School of Chemistry and Chemical Engineering, Nanjing University, Nanjing, China. [4]Key Laboratory of Theoretical and Computational Photochemistry of Ministry of Education, Department of Chemistry, Beijing Normal University, Beijing, China. [5]Department of Physics and State Key Laboratory of Luminescent Materials and Devices, South China University of Technology, Guangzhou, China. [6]Department of Physics, University of Arkansas, Fayetteville, AR, USA. [7]These authors contributed equally: Zhiwei Wang, Heyuan Liu, Xiaoyu Xie. ✉e-mail: cfzhang@nju.edu.cn; haibo@nju.edu.cn; xiyouli@upc.edu.cn; mxiao@uark.edu

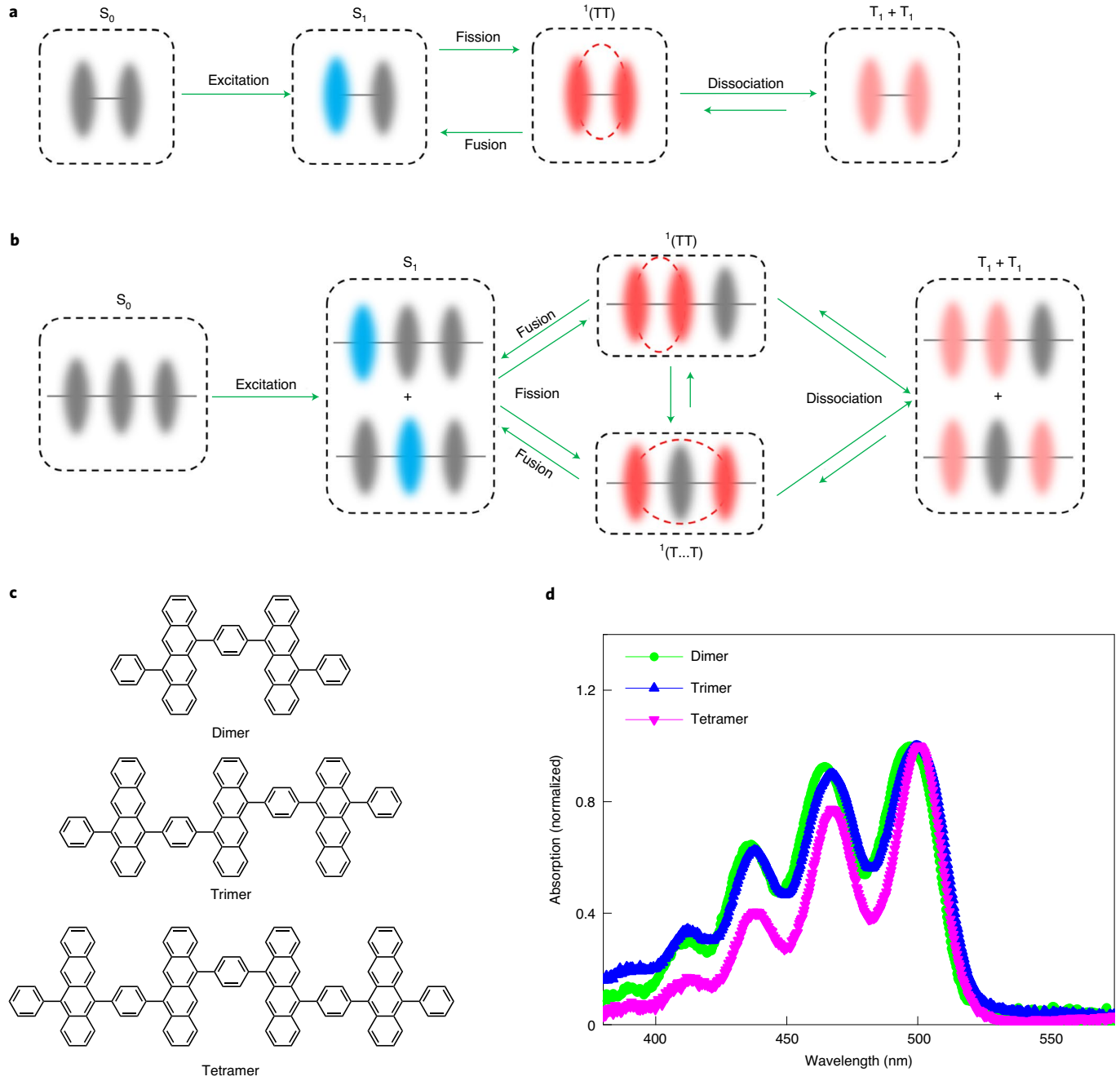

Fig. 1 | Scenarios of the iSF processes involving different intermediate states. a, Scheme of the iSF process mediated by the ^{1}(TT) state in a dimer system. **b**, Scheme of the iSF processes mediated by both the ^{1}(TT) and ^{1}(T…T) states in a trimer or larger array systems. **c**, Molecular structures of tetracene dimer, trimer and tetramer (studied in this work). **d**, Absorption spectra of toluene solutions of tetracene dimer, trimer and tetramer (studied in this work).

formation of the ^{1}(T…T) state can be largely suppressed by applying an external magnetic field (~0.8 T) whereas the formation of the ^{1}(TT) state is nearly independent of the magnetic field. In addition to the ^{1}(TT) states observed in all three oligomers, we have clearly identified a slow component for triplet generation caused by the formation of ^{1}(T…T) states in the trimer and tetramer systems by the magneto-optical measurements. Quantitative analyses indicate that the efficiencies of free-triplet generation increase from 21% in the dimer to 85% in the trimer and 124% in the tetramer. Our findings reveal a new insight into the fundamental mechanism of iSF dynamics and provide an alternative approach to achieve highly efficient free-triplet generation in iSF materials which is valuable for potential applications.

Results

Two-step iSF processes in tetracene oligomers. Figure 1c shows the molecular structures of the tetracene oligomers studied in this work. The details of the synthesis methods are reported elsewhere[33,34]. The tetracene dimer, trimer and tetramer exhibit structures with benzene-linked tetracene subunits. Their similar absorption peak positions (Fig. 1d) suggest that the chromophore units are weakly coupled. The vibronic feature in the absorption spectrum is

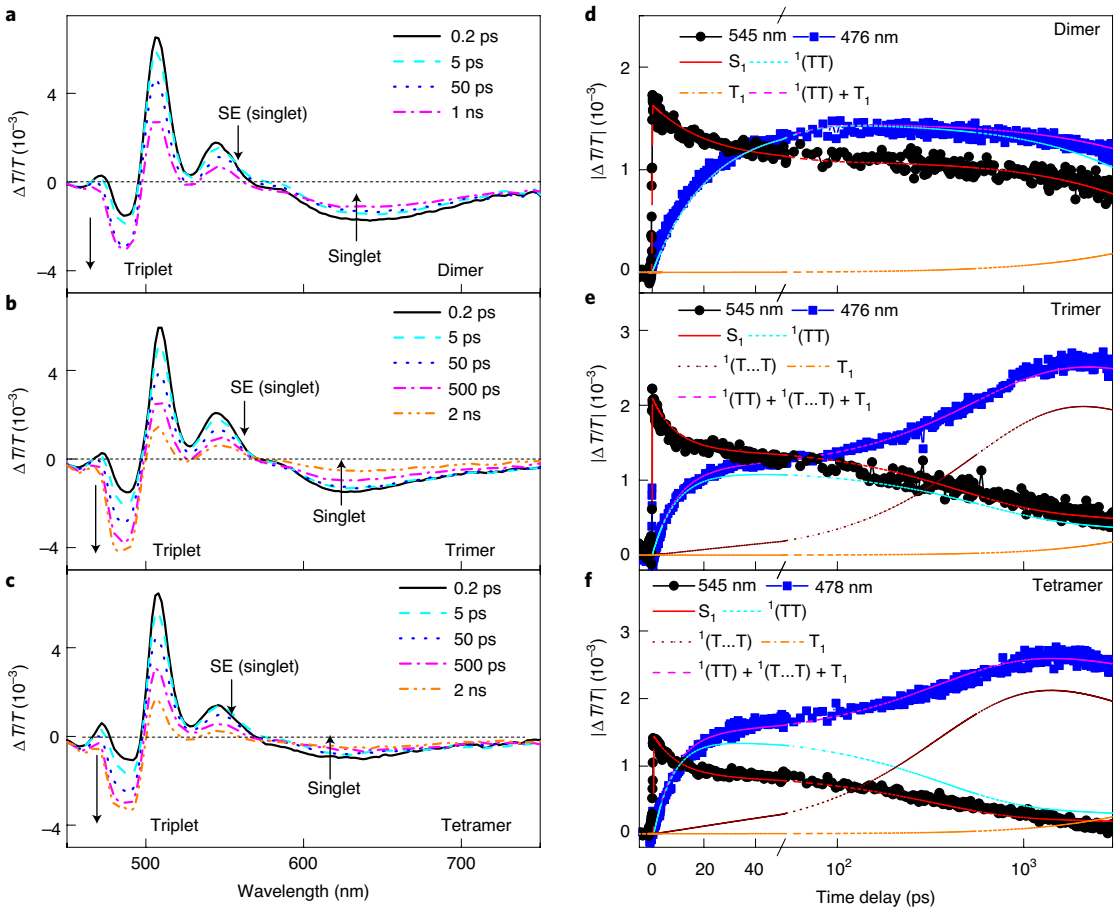

Fig. 2 | TA spectra revealing the iSF dynamics in the tetracene oligomers. a–c, Femtosecond-resolved TA spectra of the toluene solutions of the tetracene dimer (**a**), trimer (**b**) and tetramer (**c**) with pump at 470 nm. **d–f**, Kinetic curves probed at the characteristic wavelengths showing the dynamics of the singlet and triplet states in the tetracene dimer (**d**), trimer (**e**) and tetramer (**f**). The lines represent the dynamics of different species (S_1, ^{1}(TT), ^{1}(T…T), T_1 and the sum of the triplet populations) derived with the kinetic model (Fig. 1a,b) by a global fitting analysis (see Supplementary Section 3 for details).

noticeably reduced in the tetramer, implying a certain degree of delocalization for the S_1 state in long oligomers which is possibly beneficial for singlet fission[35,36].

The SF processes in these oligomers are characterized by transient absorption (TA) spectroscopy (Fig. 2). In addition to the bleach signals ($\Delta T/T > 0$) caused by ground-state bleaching (GSB) and stimulated emission (SE), two excited-state absorption (ESA) features are observed in the TA data of all three oligomers. The spectroscopic characteristics of the singlet and triplet states can be determined by triplet sensitization measurements (Supplementary Fig. 1). The trace of SE feature near 545 nm represents the dynamics of photoexcited singlet states, and the ESA feature of singlet states is observed near 636 nm and appears simultaneously upon optical pumping (Fig. 2a–c). The ESA bands of triplet populations are characterized to be near 480 nm, and partially overlap with the weak ESA signals of the singlet states at the initial stage. To extract the kinetic information about triplet generations in these oligomers, we select the probed wavelengths of 476 nm for the dimer and trimer and 478 nm for the tetramer, respectively, where the ESA and GSB signals of the singlet states are offset with the same amplitudes. The kinetic curves at these characteristic wavelengths represent the dynamics of the triplet population, which is further confirmed by the biexponential dynamics at a later stage for the processes of TTA and free-triplet recombination (Fig. 3)[11].

We carefully analyse the correlated dynamics of singlet and triplet states in the tetracene oligomers (Fig. 2d–f). Notably, two-stage growth dynamics is observed for triplet population generations in the trimer (Fig. 2e) and tetramer (Fig. 2f). The observed dynamics of triplet generation is consistent with the scenario considering two coexisting intermediate states of triplet pairs (that is, ^{1}(TT) and ^{1}(T…T) states) in the trimer and tetramer. A fast component with a lifetime of ~10 ps appears in the signals of all three samples, whereas a slow component with a lifetime of ~400 ps only exists for the trimer and tetramer. The fast and slow components can be ascribed to the generation of the ^{1}(TT) and ^{1}(T…T) states, respectively, which further dissociate into free triplets. Only the ^{1}(TT) state can be excited in the dimer, so that the slow rising component is absent in Fig. 2d. The experimental data can be well reproduced by a model considering two channels involving the ^{1}(TT) and ^{1}(T…T) states, respectively (Supplementary Fig. 2 and Supplementary Section 3).

The yields of triplet population generations are evaluated with the precalibrated molar extinction coefficients of ESA of the S_1 and T_1 states (see Supplementary Section 2 for details). The peak efficiency of triplet population increases from 59% in the dimer to 152% in the trimer and to 189% in the tetramer, which includes contributions from the ^{1}(TT), ^{1}(T…T) and free T_1 states. The recovery dynamics of the triplet signals in the tetracene oligomers exhibits biexponential decay behaviour (Fig. 3). The extremely long components with lifetimes of the order of 100 µs plausibly result from the recovery processes of free triplets in these oligomers. To evaluate the TT dissociation, we estimate the efficiencies for free-triplet generations from the signals recorded at the delay time of 100 ns (SI).

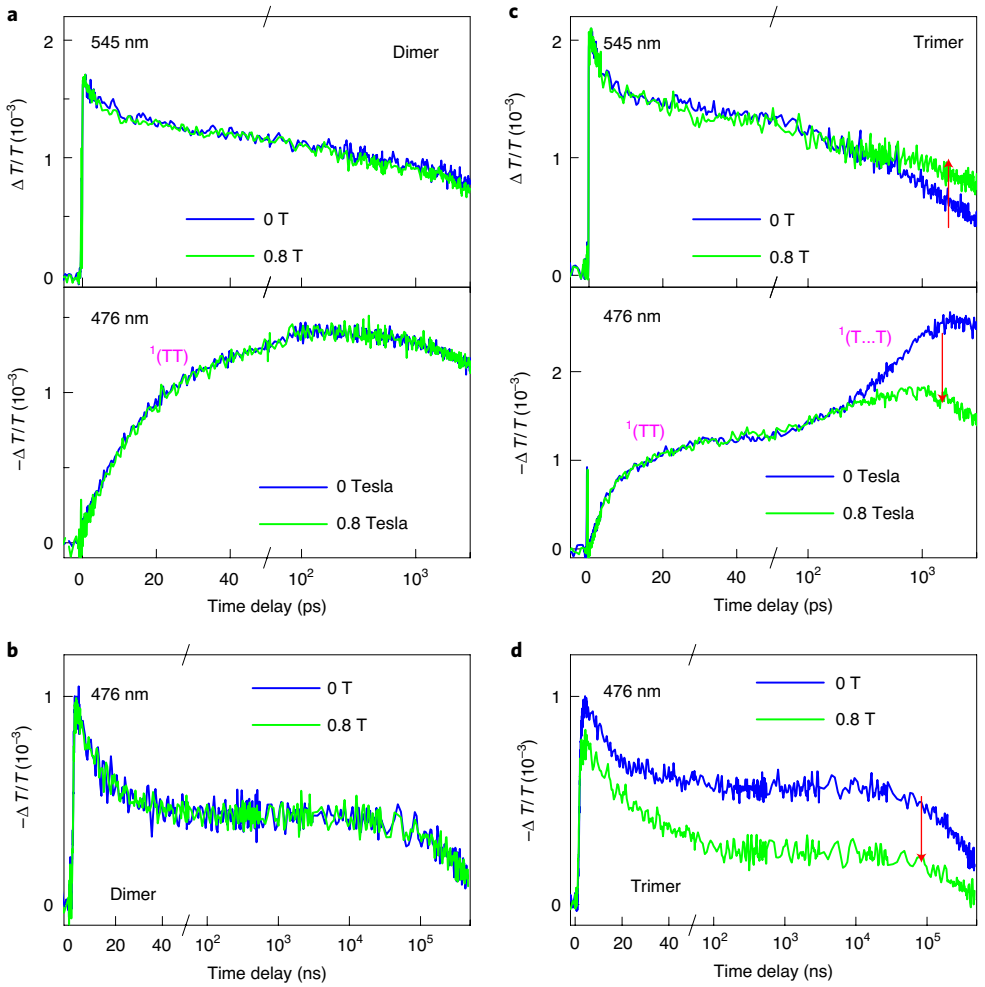

Fig. 3 | MFE on the iSF dynamics in the tetracene oligomers. Dynamics of the singlet and triplet states for toluene solutions of the tetracene dimer (**a**,**b**) and the tetracene trimer (**c**,**d**) with and without applying an external magnetic field of 0.8 T. The singlet population dynamics are probed at 545 nm and the triplet population dynamics are probed at 476 nm. In the tetracene trimer, the magnetic field suppresses the formation of the ^{1}(T…T) state, resulting in the MFEs on the excited state dynamics. The red arrows indicate the change that occurs when an external magnetic field is applied (**c**,**d**).

The values are estimated to be approximately 21%, 85% and 124% for the dimer, trimer and tetramer (Table 1), respectively, suggesting a dramatic enhancement of free-triplet generation with the increased number of tetracene units.

MFEs on the iSF processes in tetracene oligomers. To further confirm the role of the ^{1}(T…T) state in the iSF processes, we probe the iSF dynamics in the oligomers under an external magnetic field. The magnetic field affects the distributions of singlet characters of nine eigenstates of correlated triplet pairs according to the Johnson–Merrifield model[37–39], which is governed by the spin-related Hamiltonian of the triplet pair including the inter-triplet exchange and dipole interaction, zero-field splitting and the Zeeman interaction (Supplementary Section 4)[26,31,32,38,40,41]. As shown in Supplementary Fig. 6, we calculate the singlet character of each eigenstate of correlated triplet pairs as a function of the magnetic field with relatively weak and strong exchange interactions. In the relevant regime of the magnetic field (<1 T), the MFE is important for the weakly coupled triplet pairs but becomes negligible when the strength of the exchange interaction is >100 μeV. These results are consistent with previous reports where the low-field MFEs are related to the weakly coupled triplet pairs[26,31,32]. The exchange interaction for the ^{1}(TT) states has been recently quantified to be 0.3−5 meV in crystalline 5,12-bis((triisopropylsilyl) ethynyl)tetracene (TIPS-tetracene)[32], which is much larger than the Zeeman interaction with the magnetic field magnitude applied in this study (<1 T) so that the MFE for ^{1}(TT) states is weak. For the spatially separated ^{1}(T…T) states, the strength of the intertriplet exchange interaction will be markedly weaker, so that the MFE on the iSF dynamics of the ^{1}(T…T) states becomes more important and detectable.

Figure 3 compares the dynamics of the singlet and triplet states recorded in the tetracene dimer and trimer with and without applying a magnetic field of ~0.8 T. The dynamics in the tetracene dimer is nearly unchanged by the magnetic field (Fig. 3a,b). In contrast, the dynamics in the tetracene trimer (Fig. 3c,d) and tetramer (Supplementary Fig. 10) show notable magnetic field dependences for delay times >100 ps. The slow rising components of the triplet populations in the trimer and tetramer are greatly suppressed by applying an external magnetic field (Fig. 3c,d) whereas the decays of singlet population become slower (Fig. 3c). These results verify that the slower rising component is related to the formation of the ^{1}(T…T) states. With a weak exchange interaction, the dynamics of the ^{1}(T…T) states in the tetracene trimer and tetramer are much more sensitive to the Zeeman interaction induced by the external magnetic field. The dynamics in the trimer and tetramer at the early stage (<20 ps), like that in the dimer, are nearly independent of the magnetic field, confirming the generation of the adjacent ^{1}(TT)

Table 1 | Quantum efficiencies of the maximum triplet population (Φ_T), free triplet population (Φ_{T1}) and FL emission (Φ_F) for toluene solutions of the tetracene oligomers with and without an applied magnetic field of 0.8 T

Molecule	Φ_T (%)		Φ_{T1} (%)		Φ_F (%)	
	0 T	0.8 T	0 T	0.8 T	0 T	0.8 T
Dimer	59±7	59±7	21±3	21±3	65±4	65±4
Trimer	152±20	98±10	85±8	38±4	41±4	77±5
Tetramer	189±20	149±20	124±10	74±8	25±3	64±4

states with strong intertriplet coupling. The above-measured MFEs explicitly show that the ^{1}(TT) and ^{1}(T…T) states are both involved in the iSF process at different stages in these tetracene oligomers.

For more insights about the MFEs, we perform theoretical simulations on the SF kinetics involving triplet pair states with different exchange interaction strengths (Supplementary Section 4). The experimental data can be qualitatively explained with the Johnson–Merrifield model when we consider a weakly exchange-coupled triplet pair ^{1}(TT) in the dimer and an additional strongly exchange-coupled triplet pair ^{1}(T…T) in the trimer. When an external magnetic field of 0.8 T is applied, the ^{1}(TT) formation remains unchanged and the ^{1}(T…T) formation is largely suppressed (Supplementary Figs. 7 and 8). Nevertheless, the magnitude of MFE predicted by the Johnson–Merrifield model is much weaker than the experimental value, probably because the model does not consider the spin dephasing process of the correlated triplet pair (Supplementary Fig. 8). Following the approach suggested by Wakasa and co-workers[42], we simulate the kinetics by employing the spin states of the triplet pair as bases to include the spin-dephasing processes (Supplementary Figs. 8 and 9). The simulation results show better reproduction of the MFE with a certain level of dephasing rate (Supplementary Fig. 8), implying that the spin dephasing of correlated triplet pairs plays an important role in the MFE on the kinetics.

Dissociation of the ^{1}(TT) and ^{1}(T…T) states. The most intriguing potential of the ^{1}(T…T) state is its ability to dissociate into free triplets with a markedly enhanced efficiency in comparison with the ^{1}(TT) state. We analyse the different dissociation processes related to the ^{1}(TT) and ^{1}(T…T) states by studying the MFEs on the free-triplet generation. As noted above, the formation of the ^{1}(T…T) state is largely inhibited by the magnetic field, which is manifested in the magnetic field dependences of the TA and fluorescence (FL) spectra (Fig. 4). The simultaneous drop of free-triplet signal together with suppression of the formation of the ^{1}(T…T) states indicates that SF is the primary channel for free-triplet generation, which is reasonable because intersystem crossing is orders of magnitude slower in the system with weak spin–orbit coupling[43].

Figure 4a shows the TA spectra recorded at the time delay of 100 ns under an external magnetic field of different magnitudes. On this time scale, the ESA signal probed at 480 nm is mainly contributed by free triplets. In the dimer, the signal of the free triplet is nearly independent of the magnetic field, which is consistent with the fact that the MFE is only related to the ^{1}(T…T) states (Fig. 4a). In the trimer and tetramer, about 50% of the free triplets are suppressed upon applying a magnetic field of 0.8 T (Fig. 4a), confirming the important contribution of ^{1}(T…T) states to free-triplet generation. The magnetic field strongly suppresses an important removal pathway of singlet states ($S_1 \rightarrow {}^1$(T…T)), which can be also probed by FL emission (Fig. 4). The quantum yield of the FL emission increases from 41% (0 T) to 77% (0.8 T) in the trimer and from 25% (0 T) to 64% (0.8 T) in the tetramer (Table 1), respectively. These results suggest that a certain portion of the singlet population, which is originally converted into free triplets through the ^{1}(T…T) states, recombines through the radiative emission pathway with longer FL lifetime (Supplementary Fig. 12) when the magnetic field is applied.

The field-dependent TA signal and FL intensity can be roughly fitted by the Lorentzian function profile[44]. The fitted values of the full width at half maximum (FWHM) are 0.57 T for the TA signals and 0.51 T for the FL intensity of the trimer; the corresponding values for the tetramer are 0.67 and 0.63 T. The similar FWHM values for field dependences of the TA and FL signals indicate that the same mechanism is responsible for these MFEs. The corresponding strengths of the Zeeman interactions are <0.1 meV. The substantial MFEs caused by such weak Zeeman interactions in the trimer and tetramer confirm the scenario that there is a weak spin exchange coupling between the correlated triplets for the ^{1}(T…T) state.

By assuming that the MFE on free-triplet generation is solely induced by the ^{1}(T…T) state, we can estimate the dissociation efficiencies for the ^{1}(TT) and ^{1}(T…T) states to be ~40% and ~90%, respectively, in the trimer (see the Supplementary Information for the calculation details). Next, we discuss possible mechanisms responsible for the different dissociation properties of the ^{1}(TT) and ^{1}(T…T) states. For tetracene dimers with different linkers, Korovina et al[16] suggested that rotational motions of the chromophores are important for the TT dissociation. In addition, the difference in the intertriplet distance is probably the main origin since both the electronic and spin degrees of freedom are sensitive to the spatial separation of the coupled triplets. Intertriplet electronic coupling of the ^{1}(T…T) state is markedly reduced in comparison to that of the ^{1}(TT) state, which suppresses the fusion process that competes against TT dissociation. Moreover, the TTA process of two uncorrelated free triplets possibly generated at one oligomer molecule seems to be unimportant at the late stage (>100 ns), which is plausibly due to the spin dephasing process with mixing between triplet pair states having different spin characteristics (Supplementary Section 4)[15,30,45]. The weaker spin exchange coupling at the ^{1}(T…T) state is also probably beneficial for the spin-dephasing process, which is essential for competing with TTA to generate two independent triplet states[15,30,45]. The dynamics of the (T…T) states involves complicated spin-dephasing and interconversion processes between singlet and quintet sublevels. As suggested in the literature, the triplet sublevels of a triplet pair may be formed by rephasing of free triplets[30] and/or mixing by quintet sublevels[45], which is possibly responsible for the long lifetime of two triplets at single molecules. However, the spin characteristics of these states cannot be distinguished by the optical measurements used in this work. The exact dynamics of the spin-mixing processes may be captured by time-resolved electron-spin resonance experiments in future studies[15,26,30,45–47].

Generation mechanisms of the ^{1}(TT) and ^{1}(T…T) states. Next, we try to understand the generation mechanisms of the two different TT states. In general, the intermediate states of correlated triplet pairs can be generated from a singlet state (that is, $S_1 \rightleftarrows$ TT) through either a direct process driven by the electronic coupling between S_1 and TT states or an indirect process mediated by a charge-transfer (CT) state[3,13,15,17,22,48–53]. In xSF materials, the ^{1}(T…T) state has been regarded as a consequence of separation of the ^{1}(TT) state through triplet energy transfer[28,29,48] and/or a result of electronic decoherence[5,21]. To shed light on this issue, we investigate the dynamics of the ^{1}(TT) and ^{1}(T…T) states during the iSF process in oligomers dissolved in solvents with different polarities[13,17].

Figure 5 compares the TA experimental data of the trimer dissolved in either toluene or dimethyl formamidine (DMF). The dynamics of iSF show a marked dependence on the solvent polarity. A slight increase in solvent polarity causes a gradual increase in the generation rate of ^{1}(TT) states (Supplementary Fig. 14) as expected

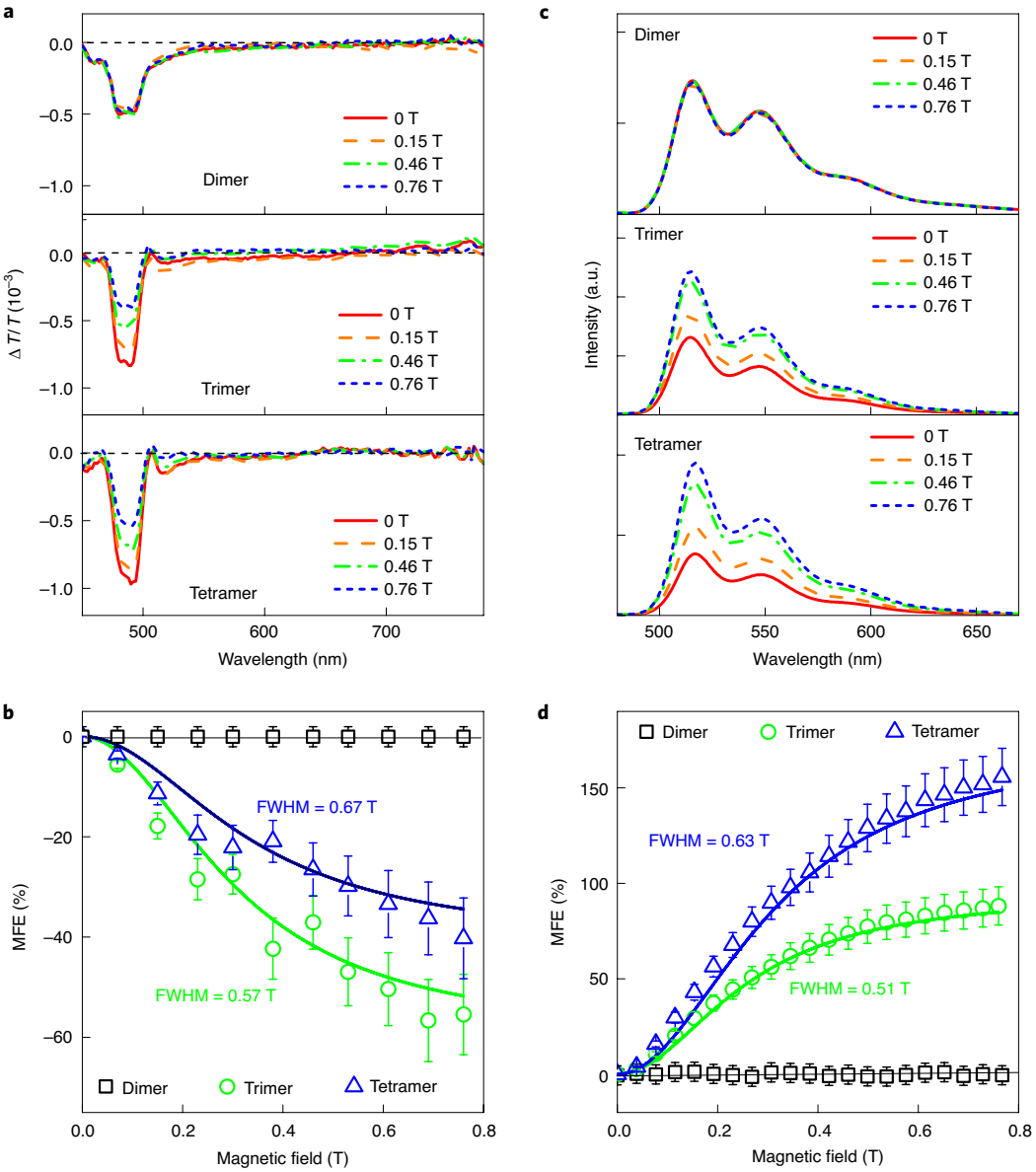

Fig. 4 | MFE on free-triplet generation in the tetracene oligomers. a, TA spectra of the tetracene oligomers recorded at a time delay of 100 ns from the tetracene oligomers while applying a magnetic field of different magnitudes. **b**, Suppressed ratios of free-triplet generation in the tetracene oligomers are plotted versus the magnitude of magnetic field. **c**, FL emission spectra of the tetracene oligomers with an applied magnetic field of different magnitudes. **d**, Enhanced ratios of FL emission in the tetracene oligomers are plotted versus the magnitude of magnetic field. Error bars represent standard deviations in the determination of the values of MFE obtained by averaging several experiments.

for a CT-mediated SF process[13,17]. When polarity further increases, the fast component of triplet generation (^{1}(TT)) is largely suppressed in DMF (Fig. 5a,b). Remarkably, for the sample dissolved in DMF, a new ESA feature emerges in the spectral range >750 nm (Fig. 5b), which is probably caused by the stabilized CT states in the solvent with a strong polarity. Similar solvent-dependent results have also been observed for the dimer and tetramer (Supplementary Figs. 15 and 16). These results are consistent with the scenario of indirect formation of the TT states through the mediation of a CT state[13,17]. In the weakly polar solvent, the energy of the CT state is much higher than those of the singlet and triplet pair states, so the CT state acts as a virtual intermediate step for the conversion from singlet to triplet pair states. In the strongly polar solvent, the energy of the CT state is lowered and the stabilized CT state is populated, as indicated by the new ESA feature (Fig. 5d). Such assignments have been confirmed by comparing the TA data in the near-infrared range with spectroelectrochemistry measurements (Supplementary Fig. 18). The spectral feature of the ESA in the DMF solution is comparable to the absorption of electrochemically introduced anions in the trimer (Supplementary Fig. 18). These corroborated experimental findings strongly support the scenario of CT-mediated iSF for the generation of ^{1}(TT) states.

Notably, the slow component of triplet generation (that is, the formation of the ^{1}(T…T) state) is less sensitive to the solvent polarity (Fig. 5c). It has been suggested that the ^{1}(T…T) state in xSF materials of crystalline polyacenes is generated as an intermediate step of ^{1}(TT) dissociation[5,21,28,29]. Such a triplet-hopping process (that is, triplet energy transfer) may be considered as a natural channel for the generation of the ^{1}(T…T) state. Nevertheless, when the formation of the ^{1}(TT) state is suppressed in DMF, the delayed

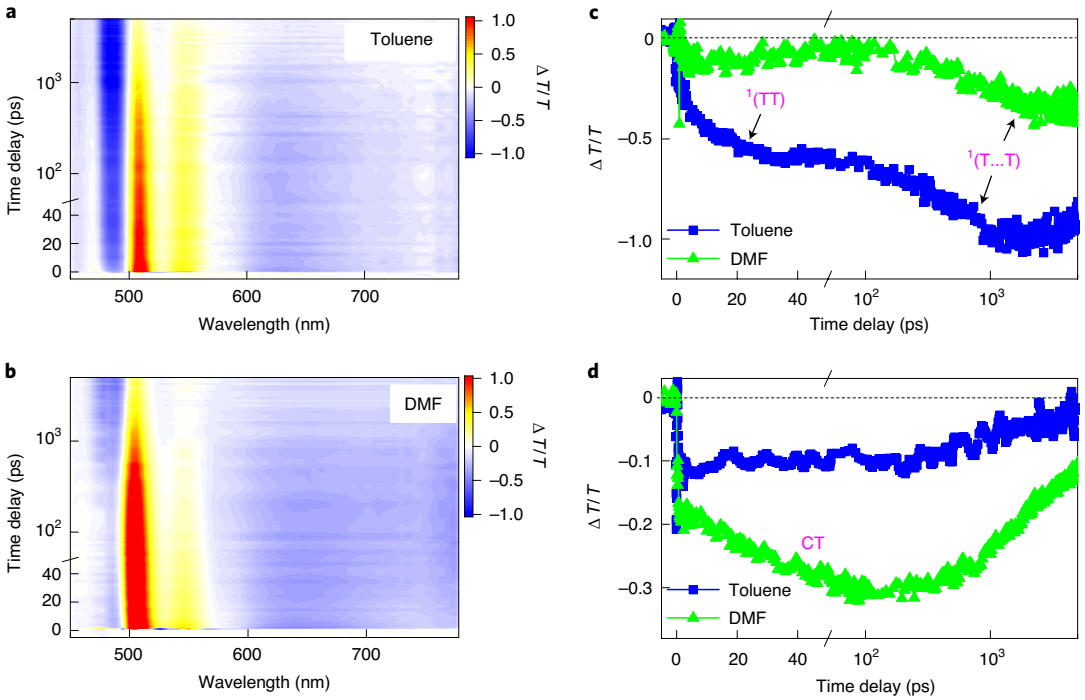

Fig. 5 | Solvent polarity effect on the iSF dynamics in the tetracene trimer. a,**b**, TA spectra of the tetracene trimer dissolved in toluene (**a**) and DMF (**b**). The data are plotted at a scale normalized to the GSB signal. The dynamic curves probed at 476 nm (**c**) and 750–775 nm (**d**) from the sample dissolved in either toluene or DMF show the formation of a stabilized CT state in the solvent with strong polarity.

rise component of the triplet signal is largely retained (Fig. 5c). This delayed rise component in DMF is further confirmed to be due to the ^{1}(T…T) state by magnetic-field-dependent measurements (Supplementary Fig. 11), suggesting the presence of another channel for the generation of the ^{1}(T…T) state in addition to the triplet hopping. Moreover, fluorescence emission from the DMF solution sample is strongly enhanced when the ^{1}(T…T) states are suppressed by a magnetic field (Supplementary Fig. 11), implying that the ^{1}(T…T) states are plausibly converted from the photoexcited S_1 states. The above experimental results strongly suggest that different from the SF process of $S_1 \rightleftarrows {}^1(TT) \rightleftarrows T_1 + T_1$ in the dimer, two channels probably exist for SF in the trimer and tetramer systems (that is, $S_1 \rightleftarrows {}^1(TT) \rightleftarrows {}^1(T\ldots T) \rightleftarrows T_1 + T_1$ and $S_1 \rightleftarrows {}^1(T\ldots T) \rightleftarrows T_1 + T_1$). A kinetic model considering the two channels has been adopted to fit the experimental data (Supplementary Section 3 and Supplementary Fig. 2) and extract the dynamics of different excited species (Fig. 2).

Next, we discuss possible microscopic mechanisms underlying the generation processes of the ^{1}(TT) and ^{1}(T…T) states in tetracene oligomers. We first survey the energy alignments and electronic coupling strengths between the diabatic electronic excited states involved in the iSF process in these oligomers by employing quantum chemical calculations (Supplementary Section 11). The strengths of direct couplings between the S_1 and ^{1}(TT) or ^{1}(T…T) states are found to be negligibly weak (Supplementary Table 6). The CT states, where the electrons and holes are located at neighbouring tetracene units (namely, short-range CT states), are found to have non-zero couplings with both the ^{1}(TT) and S_1 states for the equilibrium geometries of all three oligomers. This can well explain the fast iSF process of $S_1 \rightleftarrows {}^1(TT)$ through the mediation of the CT states (Figs. 2 and 3)[3,13,17,50,54]. In contrast, the couplings between such short-range CT states and ^{1}(T…T) states are negligibly weak, limiting the generation of ^{1}(T…T) from S_1 through such a short-range CT-mediated channel. To understand the mechanism for the slow SF channel, we further resort to studying the role of thermal fluctuations in the trimer by performing quantum chemical calculations over molecular dynamics trajectories at room temperature (Supplementary Fig. 21). For some molecular geometries distorted due to thermal fluctuation, the long-range CT states with the electron and hole located at non-neighbouring units[55], which are absent in the dimer, are found to have non-negligible couplings to the S_1 and ^{1}(T…T) states in the trimer (Supplementary Table 7). Such a long-range CT-mediated channel is possibly responsible for the slow SF process ($S_1 \rightleftarrows {}^1(T\ldots T)$). The solvent polarity dependences of the generation dynamics of the ^{1}(TT) and ^{1}(T…T) states can also be ascribed to the different energy alignments of the short- and long-range CT states with respect to the S_1 state (Supplementary Fig. 22 and Supplementary Section 11). In the highly polar DMF solution, the short-range CT state is stabilized, which suppresses the formation of the ^{1}(TT) state as observed in the dimer (Supplementary Fig. 15). Nonetheless, a portion of the S_1 population may last into the time scale of 10–100 ps (Supplementary Figs. 23 and 24). That is because CT in our systems always has a strong tendency to couple with locally excited singlet states due to their effective diabatic couplings (~50 meV; see Supplementary Table 5). Therefore, the existence of S_1 population over the energetically lower CT in polar solvents still provides sufficient initial state sources for possible singlet fission to ^{1}(T…T) according to the above-suggested mechanisms. In addition, Alvertis et al[56] recently also proposed a concept of using a destabilized 'upper' CT state as an SF intermediate in polar solvents to avoid getting trapped in lower-lying CT states. When the solvent polarity is in the regime with the long-range CT state above the S_1 state in the trimer or tetramer, the $S_1 \rightleftarrows {}^1(T\ldots T)$ channel will dramatically shift the equilibrium to (T…T) formation (Supplementary Fig. 25).

The above scenario further verifies the importance of thermal activation (or in other words, electron–vibration coupling) for SF processes[49,56–58]. The computed long-range CT-mediated couplings are found to be highly temperature dependent, increasing from vanishingly small at zero temperature to being non-negligible (0.1–0.9 meV) at room temperature (Supplementary Table 7).

This suggests that the slow iSF process for ^{1}(T…T) generation involves a thermally activated channel[49,56–58], which agrees well with the experimental results showing strong temperature dependence of the ^{1}(T…T) generation process (Supplementary Fig. 19). Temperature-dependent activation, together with the high iSF quantum yield, suggests that entropic gain probably plays an important role in the slightly endothermic generation of the ^{1}(T…T) states in the trimer and tetramer. The increased number of triplet pair sublevels and the rotational isomers[14,59] may contribute to the entropic gain to enhance the driving force for the formation of the ^{1}(T…T) states.

Conclusion

We have shown that together with the ^{1}(TT) state, the spatially separated ^{1}(T…T) state acts as an intermediate for efficient iSF processes in covalently linked tetracene trimer or larger arrays. Different from that for the ^{1}(TT) state, the generation dynamics of this weakly spin exchange coupled ^{1}(T…T) state is strongly dependent on the magnetic field. Benefiting from the weak intertriplet interaction, the triplet pair dissociation for the ^{1}(T…T) state is much more efficient than that for the ^{1}(TT) state, which promotes the efficiency of free-triplet generation from 21% for the dimer to 85% for the trimer and to 124% for the tetramer. Our results provide an alternative route for highly efficient TT dissociation, representing an important step towards practical applications of iSF materials because the free triplets can be harvested much more efficiently than the TT states through interfacial charge transfer[60].

Online content

Any methods, additional references, Nature Research reporting summaries, source data, extended data, supplementary information, acknowledgements, peer review information; details of author contributions and competing interests; and statements of data and code availability are available at https://doi.org/10.1038/s41557-021-00665-7.

Received: 26 February 2019; Accepted: 22 February 2021;
Published online: 08 April 2021

References

1. Smith, M. B. & Michl, J. Singlet fission. *Chem. Rev.* **110**, 6891–6936 (2010).
2. Smith, M. B. & Michl, J. Recent advances in singlet fission. *Annu. Rev. Phys. Chem.* **64**, 361–386 (2013).
3. Casanova, D. Theoretical modeling of singlet fission. *Chem. Rev.* **118**, 7164–7207 (2018).
4. Rao, A. & Friend, R. H. Harnessing singlet exciton fission to break the Shockley–Queisser limit. *Nat. Rev. Mater.* **2**, 17063 (2017).
5. Miyata, K., Conrad-Burton, F. S., Geyer, F. L. & Zhu, X.-Y. Triplet pair states in singlet fission. *Chem. Rev.* **119**, 4261–4292 (2019).
6. Congreve, D. N. et al. External quantum efficiency above 100% in a singlet-exciton-fission-based organic photovoltaic cell. *Science* **340**, 334–337 (2013).
7. Tayebjee, M. J. Y., Gray-Weale, A. A. & Schmidt, T. W. Thermodynamic limit of exciton fission solar cell efficiency. *J. Phys. Chem. Lett.* **3**, 2749–2754 (2012).
8. Hanna, M. C. & Nozik, A. J. Solar conversion efficiency of photovoltaic and photoelectrolysis cells with carrier multiplication absorbers. *J. Appl. Phys.* **100**, 074510 (2006).
9. Müller, A. M. et al. Exciton fission and fusion in bis(tetracene) molecules with different covalent linker structures. *J. Am. Chem. Soc.* **129**, 14240–14250 (2007).
10. Zirzlmeier, J. et al. Singlet fission in pentacene dimers. *Proc. Natl Acad. Sci. USA* **112**, 5325–5330 (2015).
11. Sanders, S. N. et al. Quantitative intramolecular singlet fission in bipentacenes. *J. Am. Chem. Soc.* **137**, 8965–8972 (2015).
12. Lukman, S. et al. Tuneable singlet exciton fission and triplet–triplet annihilation in an orthogonal pentacene dimer. *Adv. Funct. Mater.* **25**, 5452–5461 (2015).
13. Lukman, S. et al. Tuning the role of charge-transfer states in intramolecular singlet exciton fission through side-group engineering. *Nat. Commun.* **7**, 13622 (2016).
14. Korovina, N. V. et al. Singlet fission in a covalently linked cofacial alkynyltetracene dimer. *J. Am. Chem. Soc.* **138**, 617–627 (2016).
15. Basel, B. S. et al. Unified model for singlet fission within a non-conjugated covalent pentacene dimer. *Nat. Commun.* **8**, 15171 (2017).
16. Korovina, N. V. et al. Linker-dependent singlet fission in tetracene dimers. *J. Am. Chem. Soc.* **140**, 10179–10190 (2018).
17. Margulies, E. A. et al. Enabling singlet fission by controlling intramolecular charge transfer in π-stacked covalent terrylenediimide dimers. *Nat. Chem.* **8**, 1120–1125 (2016).
18. Sung, J. et al. Direct observation of excimer-mediated intramolecular electron transfer in a cofacially-stacked perylene bisimide pair. *J. Am. Chem. Soc.* **138**, 9029–9032 (2016).
19. Kumarasamy, E. et al. Tuning singlet fission in π-bridge-π chromophores. *J. Am. Chem. Soc.* **139**, 12488–12494 (2017).
20. Busby, E. et al. A design strategy for intramolecular singlet fission mediated by charge-transfer states in donor–acceptor organic materials. *Nat. Mater.* **14**, 426–433 (2015).
21. Chan, W.-L. et al. Observing the multiexciton state in singlet fission and ensuing ultrafast multielectron transfer. *Science* **334**, 1541–1545 (2011).
22. Zimmerman, P. M., Zhang, Z. & Musgrave, C. B. Singlet fission in pentacene through multi-exciton quantum states. *Nat. Chem.* **2**, 648–652 (2010).
23. Pace, N. A. et al. Controlling long-lived triplet generation from intramolecular singlet fission in the solid state. *J. Phys. Chem. Lett.* **8**, 6086–6091 (2017).
24. Schrauben, J. N. et al. Excitation localization/delocalization isomerism in a strongly coupled covalent dimer of 1,3-diphenylisobenzofuran. *J. Phys. Chem. A* **120**, 3473–3483 (2016).
25. Wu, Y. et al. Intramolecular singlet fission in an antiaromatic polycyclic hydrocarbon. *Angew. Chem. Int. Ed.* **56**, 9400–9404 (2017).
26. Wakasa, M. et al. What can be learned from magnetic field effects on singlet fission: role of exchange interaction in excited triplet pairs. *J. Phys. Chem. C* **119**, 25840–25844 (2015).
27. Wan, Y. et al. Cooperative singlet and triplet exciton transport in tetracene crystals visualized by ultrafast microscopy. *Nat. Chem.* **7**, 785–792 (2015).
28. Pensack, R. D. et al. Observation of two triplet-pair intermediates in singlet exciton fission. *J. Phys. Chem. Lett.* **7**, 2370–2375 (2016).
29. Breen, I. et al. Triplet separation drives singlet fission after femtosecond correlated triplet pair production in rubrene. *J. Am. Chem. Soc.* **139**, 11745–11751 (2017).
30. Pun, A. B. et al. Ultrafast intramolecular singlet fission to persistent multiexcitons by molecular design. *Nat. Chem.* **11**, 821–828 (2019).
31. Bayliss, S. L. et al. Spin signatures of exchange-coupled triplet pairs formed by singlet fission. *Phys. Rev. B* **94**, 045204 (2016).
32. Bayliss, S. L. et al. Site-selective measurement of coupled spin pairs in an organic semiconductor. *Proc. Natl Acad. Sci. USA* **115**, 5077–5082 (2018).
33. Liu, H. et al. A covalently linked tetracene trimer: synthesis and singlet exciton fission property. *Org. Lett.* **19**, 580–583 (2017).
34. Wang, X. et al. Intramolecular singlet fission in a face-to-face stacked tetracene trimer. *Phys. Chem. Chem. Phys.* **20**, 6330–6336 (2018).
35. Pensack, R. D. et al. Exciton delocalization drives rapid singlet fission in nanoparticles of acene derivatives. *J. Am. Chem. Soc.* **137**, 6790–6803 (2015).
36. Pun, A. B. et al. Triplet harvesting from intramolecular singlet fission in polytetracene. *Adv. Mater.* **29**, 1701416 (2017).
37. Johnson, J. C. & Merrifield, R. E. Effects of magentic fields on the mutual annihilation of triplet excitons in anthracene crystals. *Phys. Rev. B* **1**, 896–902 (1970).
38. Burdett, J. J., Piland, G. B. & Bardeen, C. J. Magnetic field effects and the role of spin states in singlet fission. *Chem. Phys. Lett.* **585**, 1–10 (2013).
39. Johnson, R. C., Merrifield, R. E., Avakian, P. & Flippen, R. B. Effects of magnetic fields on mutual annihilation of triplet excitons in molecular crystals. *Phys. Rev. Lett.* **19**, 285–287 (1967).
40. Bayliss, S. L. et al. Geminate and nongeminate recombination of triplet excitons formed by singlet fission. *Phys. Rev. Lett.* **112**, 238701 (2014).
41. Wang, R. et al. Magnetic dipolar interaction between correlated triplets created by singlet fission in tetracene crystals. *Nat. Commun.* **6**, 8602 (2015).
42. Yago, T., Ishikawa, K., Katoh, R. & Wakasa, M. Magnetic field effects on triplet pair generated by singlet fission in an organic crystal: application of radical pair model to triplet pair. *J. Phys. Chem. C* **120**, 27858–27870 (2016).
43. Roberts, S. T. et al. Efficient singlet fission discovered in a disordered acene film. *J. Am. Chem. Soc.* **134**, 6388–6400 (2012).
44. Devir-Wolfman, A. H. et al. Short-lived charge-transfer excitons in organic photovoltaic cells studied by high-field magneto-photocurrent. *Nat. Commun.* **5**, 4529 (2014).
45. Chen, M. et al. Quintet-triplet mixing determines the fate of the multiexciton state produced by singlet fission in a terrylenediimide dimer at room temperature. *Proc. Natl Acad. Sci. USA* **116**, 8178–8183 (2019).
46. Weiss, L. R. et al. Strongly exchange-coupled triplet pairs in an organic semiconductor. *Nat. Phys.* **13**, 176–181 (2016).
47. Tayebjee, M. J. Y. et al. Quintet multiexciton dynamics in singlet fission. *Nat. Phys.* **13**, 182–188 (2016).

48. Stern, H. L. et al. Vibronically coherent ultrafast triplet-pair formation and subsequent thermally activated dissociation control efficient endothermic singlet fission. *Nat. Chem.* **9**, 1205–1212 (2017).
49. Miyata, K. et al. Coherent singlet fission activated by symmetry breaking. *Nat. Chem.* **9**, 983–989 (2017).
50. Dover, C. B. et al. Endothermic singlet fission is hindered by excimer formation. *Nat. Chem.* **10**, 305–310 (2018).
51. Bakulin, A. A. et al. Real-time observation of multiexcitonic states in ultrafast singlet fission using coherent 2D electronic spectroscopy. *Nat. Chem.* **8**, 16–23 (2016).
52. Yost, S. R. et al. A transferable model for singlet-fission kinetics. *Nat. Chem.* **6**, 492–497 (2014).
53. Le, A. K. et al. Singlet fission involves an interplay between energetic driving force and electronic coupling in perylenediimide films. *J. Am. Chem. Soc.* **140**, 814–826 (2018).
54. Berkelbach, T. C., Hybertsen, M. S. & Reichman, D. R. Microscopic theory of singlet exciton fission. II. Application to pentacene dimers and the role of superexchange. *J. Chem. Phys.* **138**, 114102 (2013).
55. Ambrosio, F. & Troisi, A. Singlet fission in linear chains of molecules. *J. Chem. Phys.* **141**, 204703 (2014).
56. Alvertis, A. M. et al. Switching between coherent and incoherent singlet fission via solvent-induced symmetry breaking. *J. Am. Chem. Soc.* **141**, 17558–17570 (2019).
57. Tamura, H. et al. First-principles quantum dynamics of singlet fission: coherent versus thermally activated mechanisms governed by molecular pi stacking. *Phys. Rev. Lett.* **115**, 107401 (2015).
58. Xie, X. et al. Exciton–phonon interaction model for singlet fission in prototypical molecular crystals. *J. Chem. Theory Comput.* **15**, 3721–3729 (2019).
59. Korovina, N. V., Chang, C. H. & Johnson, J. C. Spatial separation of triplet excitons drives endothermic singlet fission. *Nat. Chem.* **12**, 391–398 (2020).
60. Trinh, M. T. et al. Distinct properties of the triplet pair state from singlet fission. *Sci. Adv.* **3**, e1700241 (2017).

Methods

Sample preparation. Synthesizing methods of the tetracene oligomers have been reported elsewhere[33,34]. For all optical measurements, the samples were dissolved in degassed toluene at concentrations of around 2×10^{-5} M. The solutions were prepared in quartz cells in an oxygen-free environment. Unless otherwise specified, optical experiments were performed at room temperature.

Optical characterization. To record the steady-state and time-resolved emission spectra, we used a 405 nm laser (Picoquant, LDC-D-C-405). The emission spectra were recorded with a spectrometer equipped with a liquid-nitrogen-cooled silicon charge-coupled device (CCD) (400BR_eXcelon, PyLoN, Princeton Instruments). Time-resolved fluorescence spectra were recorded by the technique of time-correlated single-photon counting (Picoquant, Picoharp 300) using an avalanche photodiode with a temporal resolution of ~50 ps (Picoquant, MPD)[41].

A titanium:sapphire regenerative amplifier (90 fs, 1 kHz; Libra, Coherent) was used for TA spectroscopy[61]. An optical parametric amplifier (OperA Solo, Coherent) pumped by the regenerative amplifier was used to generate the pump beam at the wavelength of 470 nm. The pump fluence was kept at ~20 μJ cm^{-2}, which is in the linear regime. The probe beam was a broadband supercontinuum light source generated by focusing a small portion of the femtosecond laser beam onto a 3-mm-thick sapphire plate. The chirp of the supercontinuum probe was corrected with an error within 100 fs over the entire spectral range. The TA signal was then analysed by a silicon CCD (S11071, Hamamatsu) mounted on a monochromator (Acton 2358, Princeton Instrument) at 1 kHz enabled by a custom-built control board from Entwicklungsbuero Stresing. The signal-to-noise ratio in differential transmission was better than 10^{-4} after accumulating and averaging 1,000 pump-on and pump-off shots for each data point. For nanosecond TA spectroscopy, we replaced the femtosecond pump beam with a frequency-tripled sub-nanosecond laser (Picolo AOT MOPA, InnoLas) at 355 nm (pulse duration, ~0.8 ns). The laser was synchronized to the probe pulse with a desired delay by an electronic delay generator (SRS DG645, Stanford Research System). The probe beam and data recording procedure were the same as used for femtosecond-resolved TA spectroscopy.

Magnetic field alignment. For the magnetic-field-dependent experiments, we used a precalibrated magnetic coil driven by a d.c. power supply. The field direction was perpendicular to the horizontal plane. The field magnitude was tuned by the applied current with an accuracy better than 0.02% (equivalent to 0.2 G at the field magnitude of 1,000 G).

Quantum chemical computation. We first performed density functional theory calculations to optimize the molecular geometries and then investigated the geometric fluctuations at room temperature by molecular dynamics simulation. Electronic structure calculations by complete active space configuration interaction and complete active space self-consistent field calculations were further implemented to uncover the different natures of the adiabatic or diabatic electronic excited states directly and indirectly involved in iSF as well as the electronic couplings between these states. Moreover, the solvent effects and the role of CT states were computed by using the solvation model based on density and constrained density functional theory. To understand the ultrafast iSF dynamics of the dimer in polar solvents, we performed non-adiabatic excited state dynamics simulation using Redfield quantum dissipation theory. Additional computational details are provided in Supplementary Section 11.

Data availability

The data shown in the paper are available from the figshare repository at https://doi.org/10.6084/m9.figshare.13669820.

References

61. Wang, R. et al. Ultrafast hole transfer mediated by polaron pairs in all-polymer photovaltaic blends. *Nat. Commun.* **10**, 398 (2019).

Acknowledgements

This work was supported by the National Key R&D Program of China (2017YFA0303703 and 2018YFA0209100), the National Natural Science Foundation of China (21922302, 21873047, 91850105, 91833305, 21722302 and 21673109), Jiangsu Provincial Funds for Distinguished Young Scientists (BK20160019), the Priority Academic Program Development of Jiangsu Higher Education Institutions (PAPD) and the Fundamental Research Funds for the Central Universities (0204-14380126). C.Z. acknowledges financial support from the Tang Scholar programme. We thank X. Wu for technical assistance. We are grateful to the High-Performance Computing Center of Nanjing University for performing the numerical calculations in this paper on its blade cluster system.

Author contributions

C.Z. and M.X. initiated the project. Z.W., R.W. and L.C. performed the optical experiments. H.L. and X.L. synthesized the molecules. C.Z., Z.W. and X.W. analysed the data. Y.X., H.M., X.X., W.F. and Y.Y. performed the quantum chemical calculations. C.Z., Z.W. and M.X. co-wrote the manuscript with help from all the other authors.

Competing interests

The authors declare no competing interests.

Additional information

Supplementary information The online version contains supplementary material available at https://doi.org/10.1038/s41557-021-00665-7.

Correspondence and requests for materials should be addressed to C.Z., H.M., X.L. or M.X.

Peer review information *Nature Chemistry* thanks T. Schmidt and the other, anonymous, reviewer(s) for their contribution to the peer review of this work.

Reprints and permissions information is available at www.nature.com/reprints.